**An Acad Bras Cienc (2023) 95(3): e20221023 DOI 10.1590/0001-3765202320221023**
Anais da Academia Brasileira de Ciências | *Annals of the Brazilian Academy of Sciences*
Printed ISSN 0001-3765 I Online ISSN 1678-2690
www.scielo.br/aabc | www.fb.com/aabcjournal

**BIOMEDICAL SCIENCES**

# Preparation, optimization and evaluation of Osthole transdermal therapeutic system

MUHAMMAD NAEEM, TANIYA IQBAL, MUHAMMAD YOUSUF, ZARQA NAWAZ, SAJJAD HUSSAIN, ABDULHAKEEM S. ALAMRI, CHARIS M. GALANAKIS & ATIF ALI

**Abstract:** In the current study, the solubility and permeability of Osthole-loaded microemulsion were enhanced, which increased bioavailability. In addition, Carbomer 940 was added for prolonged drug delivery. The microemulsion was prepared after the screening of Kukui oil, Labrasol (surfactant), and transcutol-P (co-surfactant). Pseudoternary phase diagrams were employed to find the microemulsion region. Box Behnken Design (BBD) was employed for optimizing microemulsions. Variables were related and compared using mathematical equations and response surface plots (RSP). MEBG was then compared with control gel on the basis of stability studies, drug permeation, skin irritation studies, and anti-inflammatory studies. Microemulsion preparations depicted a pH of 5.27 - 5.80, a conductivity of 139 - 185 µS/cm, a poly-dispersity index of 0.116 - 0.388, a refractive index of 1.330 - 1.427, an average droplet size of 64 - 89 nm, homogeneity, spherical shape, viscosity 52 - 185 cP. Predicted values of Optimized microemulsions showed more reasonable agreement than experimental values. The microemulsion was stable and non-irritating on Rabbit skin. MEBG showed a significant difference from control gel for percent edema inhibition from the standard. The permeation enhancing capability of MEBG using a suitable viscosity fabricates it promising carrier for transdermal delivery of Osthole.

**Key words:** Osthole, microemulsion, Kukui oil, BBD, permeation, edema.

## INTRODUCTION

The substance Osthole is extracted from annual herb fruit in the family Umbelliferae, and it has a yearly herb yellow green to white crystalline powder appearance. It belongs to the coumarin compound. Its chemical name is 7-methoxy-8-isopentenyl coumarin, its molecular weight is 244.29 and its molecular formula is $C_{15}H_{16}O_3$. It depicted antispasmodic, anti-arrhythmic, antihypertensive, antitumor effects, anti-inflammatory and immune-enhancing functions (You et al. 2009, Liao et al. 2010).

The microemulsion is a single, optically isotropic, thermodynamically stable liquid solution, with a droplet between 10 and 100 nm. It comprises the oil phase, a surfactant, a cosurfactant and an aqueous phase that is transparent, translucent and thermodynamically stable. The microemulsion merits include enhanced solubility and bioavailability by increasing its shelf life. The benefits of transdermal administration of microemulsion comprise an enhancement in drug concentration upon the skin that increases drug concentration in preparation. Secondly, an improved drug thermodynamic activity may enable its skin distribution, which is helpful for transdermal absorption. Moreover, microemulsion components can facilitate penetration enhancers by reducing the stratum corneum (SC) diffusion barrier and enhancing

the rate of drug penetration across the skin (Zhu et al. 2009, Lawrence & Rees 2000).

Transdermal delivery is a potential route of administration. Ointments, Gels, etc., cannot permeate across the skin due to the skin barrier nature of the stratum corneum. However, subcutaneous delivery is painful for penetration to skin depths. The microemulsion is considered a new drug carrier system that can effectively permeate the skin for drug delivery (Chen et al. 2007).

Microemulsions are applied transdermally to enhance the drug's bioavailability and minimize the occurrence of adverse reactions compared to oral products. Despite that, high fluidity and microemulsions limit the release and the absorption of drug. Consequently, MEBG was formulated to increase the absorption and bioavailability of the drug (Chen et al. 2006).

Response Surface Methodology is the optimization of independent variables for estimating dependent variables using BBD for creating polynomial equations by $1^{st}$, $2^{nd}$ and quadratic models. It demands little time and experimentation than needed for manufacturing conventional dosage forms. It comprises $Q_{24}$, flux and lag time-dependent variables, and oil, Smix, and water) independent variables (Box & Behnken 1960, Gannu et al. 2010).

The current study successfully prepares a new oil/water gel base containing microemulsion for Osthole transdermal delivery to enhance systemic bioavailability by increasing solubility, reducing oral gastric toxicity, and improving permeability. First, BBD was employed for optimizing independent variables via estimating dependent variables. Then, atomic force microscopy (AFM) forms were characterized, pH, zeta potential and size, viscosity, skin irritation, conductivity, refractive index and stability. Further, optimized formulations were compared for in *vitro* release/permeation and anti-inflammatory studies from control.

## MATERIALS AND METHODS

### Experimental

Osthole was purchased from YuanYe Biological Technology Co. Ltd. (Shanghai, China), Kukui oil, soybean oil, sesame oil, sunflower oil, eucalyptus oil, oleic acid, isopropyl myristate, castor oil, almond oil, olive oil, nutmeg oil, tween 20, tween 80, isopropanol, ethanol, propylene glycol were obtained from Merck, Germany.

### Screening of microemulsion components

Microemulsion components were screened by mixing Osthole 100 mg with 6mL of oils, surfactants, co-surfactants and water, separately. Drug solubility in Phosphate buffer solution (PBS) pH 7.4 was also checked. A hot plate magnetic stirrer (VelpScienifca, Germany) was used at ambient temperature for 48 hours to mix the mixture. Centrifugation (Centrifuge Machine, Hettich, Germany) was conducted for every mixture individually for 15 minutes at 10,000 RPM and then filtered through a cellulose acetate membrane filter (Sartorius, Germany) having a 0.45 µm pore size to obtain a supernatant. Solubilized Osthole concentration was analyzed at 322 nm using a UV spectrophotometer (IRMECO GmbH, Germany). Osthole concentration was investigated drawing a calibration curve modeled by linear regression equation ($R^2 = 0.999$).

$$y = 0.048x + 0.001$$

Where y is estimated for absorbance, x is calculated for concentration, 0.048 shows slope and 0.001 represent intercept.

## Construction of Pseudoternary phase diagram for microemulsions

Selected microemulsion components Kukui oil, Labrasol, Transcutol-P and water after solubility studies were used for constructing Pseudoternary phase diagrams using the water titration method for getting components concentration ranges for preparing microemulsons. Surfactant to co-surfactant weight ratios was assorted as 1:1, 2:1, and 3:1. Fixed surfactant to co-surfactant ($S_{mix}$) weight ratio was mixed with oil at a ratio of 1:9, 1:8, 1:7, 1:6, 1:5, 1:4, 1:3.5, 1:3, 1:2.33, 1:2, 1:1.5, 1:1, 1:0.67, 1:0.43, 1:0.2 and 1:0.11 for each pseudoternary phase diagram (Sahoo et al. 2014). Water was added drop-wise into each mixture of oil and Smix under magnetic stirring at ambient temperature. As a result, the mixture became clear and transparent. Pseudoternary phase diagrams were constructed to find out the optimum ranges of microemulsion components Figure 1(a,b,c).

## Response surface methodology of microemulsions

Response surface methodology (RSM) is dependent on statistical and mathematical techniques groups. It is employed for comparing the suitable functional relationship between variables (input and output). RSM has two models at 1st and 2nd degree. 1st order designs comprised 2k factorial (k its control variables number) simple design and Placket Burman. In addition, central composite (3k factorial) and BBD have frequently employed methods at $2^{nd}$-order degrees (Khuri & Mukhopadhyay 2010, Jensen 2017).

## RSM using Box Behnken Design for optimization

Box and Behnken introduced BBD, which was utilized for industrial research. Independent variables concentrations were consumed at low (-1) and high (+1) levels for optimizing oil ($X_1$), Smix ($X_2$), and water ($X_3$) that creating 17 possible runs for preparing microemulsions. In addition, three dependent variables, $Q_{24}$ ($Y_1$), flux ($Y_2$), and lag time ($Y_3$), were employed (Gannu & Rao 2012).

## Experimental Design

### *Independent and dependent variables*

Franz diffusion cell was used to perform *in vitro* permeation study of suggested 17 runs of microemulsions to calculate values of dependent variables. BBD was used to evaluate the main effects, interaction effects and quadratic effects on dependent variables. Design expert software was used to construct $1^{st}$, $2^{nd}$ and quadratic models. This design was specifically chosen because it requires fewer runs as compared to central composite design as in the case of three or four variables. This

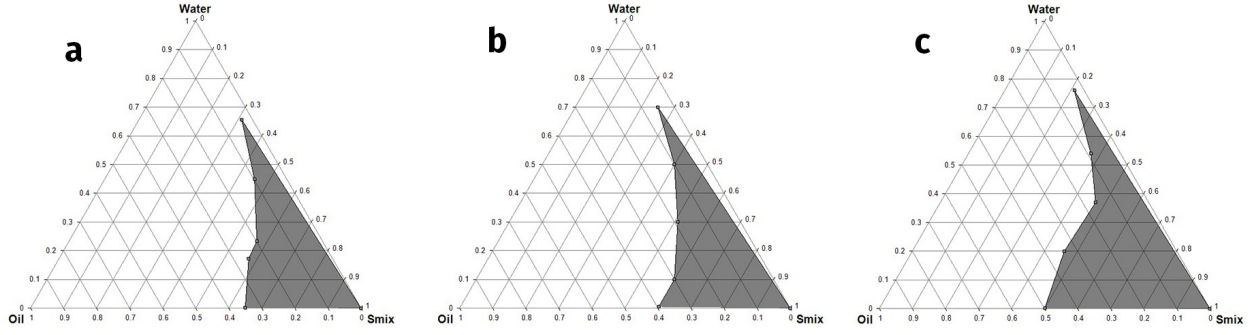


**Figure 1.** **Pseudoternary phase diagrams of microemulsions using Smix at weight ratio a) 1:1 b) 2:1 and c) 3:1.**

cubic design is characterized by points set at the midpoint of each edge and the central point of a multi-dimensional cube. Design expert software was used to generate nonlinear quadratic model equation and represented as: ($Y = b_0 + b_1X_1 + b_2X_2 + b_3X_3 + b_{12}X_1X_2 + b_{13}X_1X_3 + b_{23}X_2X_3 + b_{11}X^2_1 + b_{22}X^2_2 + b_{33}X^2_3$) (Gannu et al. 2010).

### *Checkpoint analysis and optimization model validation of microemulsion*

SPSS software used the ANOVA for validation of polynomial equations. The model was investigated for $R^2$, adjusted $R^2$, predicted $R^2$ and adequate precision. Feasibility and grid searches were performed to find out the optimum points. This software was also employed for generating many 3D response surface plots. Ten optimum check-point runs were used for the validation of polynomial equations using experimental models onto the complete experimental region via intensive grid search. Ten checkpoint preparations, Response surface characteristics were determined for each factor. Percentage prediction error was determined by correlating experimental and predicted values (Gannu & Rao 2012).

### Preparation of Osthole loaded microemulsions and PBS

Microemulsions of all 17 possible runs were prepared using the procedure: Smix was prepared by mixing Labrasol and Transcutol-P, surfactant and co-surfactant, respectively. Afterwards, Kukui oil was combined with the mixture of Smix. Next, Osthole was added at a 2% concentration to the above-prepared mixture using Ultra-Sonication (Elma, Germany). Finally, water was mixed drop by drop into the mixture with magnetic stirring moderately using ambient temperature to fabricate microemulsion (oil in water).

Control for comparison was developed as follows: In the first step, PBS (pH 7.4) was developed after mixing 0.2 M sodium hydroxide solutions and 0.2 M potassium di-hydrogen phosphate. In the second step, Osthole was mixed for preparing Osthole loaded PBS at ambient temperature using moderate magnetic stirring.

### Preparation of Osthole loaded MEBG and control gel

Carbomer 940 was used at concentrations of 0.50%, 0.75%, and 1.00% individually to prepare gel bases using a quantity sufficient (q.s) of distilled water. Afterwards the mixture dispersion was placed over-night (24 h). Thereby the polymer gel network formed after swelling. Next, Triethylamine (TEA) was mixed drop by drop until semisolid gel-like consistency was attained. pH was within 6–8 at the stage of a gel consistency. Then, the optimized preparation of Osthole microemulsion $ME_1$ was slowly mixed with Carbomer 940 at 0.75% gel base using moderate magnetic stirring. Control gel was also prepared by incorporating Osthole PBS with a 0.75% gel base.

### Characterization

A pH meter (WTW in-lab, Germany) was employed for pH measurement. Microemulsion viscosities were determined using Brookfield RVDV III ultra, Programmable Rheometer (Brookfield Engineering Laboratories, Middleboro, MA) at 25 °C. Conductivities ($\sigma$) were determined using Conductometer WTW Cond 197i Weilhein, Germany) at 25 °C. The refractive index was calculated by using BallinghamStanely (RFM 330 plus).

Optimized $ME_1$ was characterized for droplet size and poly-dispersity index using a Zeta sizer with dynamic light scattering method (Malvern Nano-ZS, UK). The shape and morphology of

Micromeulsions were measured using atomic force microscopy (AFM, XE-100, PSIA, Korea). Triplicate analysis was conducted for each preparation.

## Permeation study

### *Preparation of skin*

The study was approved by Advanced Study and Research Board (ASARB) of The Islamia University of Bahawalpur - Pakistan. Approximately 2.5 kg of male rabbit was taken to separate skin for permeation studies. Hairs trimmed carefully at Rabbit dorsal region using an electric clipper. Then, the rabbit was sacrificed, and the skin was separated from the dorsal area. The epidermis was prepared using the heat separation technique (Naeem et al. 2019). To isolate the adhered tissue, the skin was soaked at 60°C for 45 sec in PBS, pH 7.4. After that, water was used to wash the skin and cut in 1.767cm$^2$ surface area and employed for conducting *in vitro* permeation studies.

### *In Vitro permeation study microemulsions*

Drug transport through the skin is considered a very challenging and critical phenomenon for transdermal and dermal drug delivery systems. Franz diffusion cell (PermeGear, USA) surface area is 1.767 cm$^2$. It comprises two compartments (donor and receiver). Excised skin was strongly clamped between two donor and receiver compartments. The *stratum corneum* was facing the donor compartments upper side. Microemulsion was added to the donor compartment, and aluminum foil was used for covering to prevent evaporation. The receiver compartment (12 mL volume capacity) was then loaded using PBS pH 7.4 and 5% propylene glycol (PG) (its purpose is to achieve sinks conditions. Bubble formation was prevented by degassing the mixture. It also has Teflon coated magnetic stirrer for agitating the receiver compartment contents over a hot plate magnetic stirrer. The receiver compartment temperature was retained at a temperature of 37 ± 0.5°C by a water bath. Then a peristaltic pump was employed as a mechanical pump that created the pressure with tube constriction movements, as compared to natural peristalsis. At predetermined time intervals (0, 1, 2, 3, 4, 5, 6, 8, 10, 12, 14, 16, 20, and 24 hrs) sampling was conducted from receiver compartment. First, the lost quantity was refilled using equal PBS and 5% PG. Afterwards samples were diluted and then analyzed at 322nm using UV spectrophotometer (IRMECO GmbH, Germany) (Naeem et al. 2017).

### *Permeation data analysis*

The osthole cumulative amount permeated ($Q_{24}$) was measured and thereby concentration was rectified for sampling effects as reported by the following equation relation:

$$C^1_n = C_n (V_T / V_T - V_S) (C^1_{n-1} / C_{n-1})$$

Where $C^1_n$ and $C_n$ are the rectified and determined Osthole concentrations at sample $n^{th}$, respectively. $C^1_{n-1}$ is determined Osthole concentration in the sample $(n-1)^{th}$, $V_T$ and $V_S$ are the receiver fluid volume and the drawn sample, respectively.

Permeation profile was investigated using a graph between $Q_{24}$ versus time. Linear regression analysis was constructed for calculating Osthole steady-state flux ($J_{ss}$, μg/cm$^2$/hr). Lag time was calculated using intercept of time axis for plot between $Q_{24}$ (Y-axis) versus time (X-axis).

The permeability coefficient ($K_p$) was determined using the flux ratio over drug concentration in microemulsion. The Enhancement ratio (Er) was calculated by dividing microemulsion flux over control flux (Naeem et al. 2013).

### Stability studies

Stability studies were conducted for optimized $ME_1$ and MEBG. Centrifugation (Helttich, Germany) was conducted over 3500 r/m for 30 minutes. Ultra-low temperature freezer (Sanyo, Japan) was used to perform three freeze-thaw cycles. Microemulsions were stored in amber-colored containers at 40 ± 2°C/75 ± 5% RH (Relative Humidity) for 6 months. Samples were extracted at pre-determined time intervals (1, 2, 3 and 6 months) and analyzed for visual clarity, transparency, color change, phase separation, non-grittiness and drug content (Aggarwal et al. 2013).

### Skin irritation study of MEBG

Mexameter (from Courage and Khazaka Electronic GmbH, Cologne, Germany) was employed for quantifying skin erythema. Skin irritation studies were conducted on six Rabbits. Dorsal hairs were then trimmed using an electric shaver. Finally, MEBG was applied and tightened using stretch adhesive tape (Paragon™) and analyzed for erythema development for one week (Naeem et al. 2015).

### Anti-inflammatory study

Anti-inflammatory studies were performed using Rabbits after their three groups division, each group containing six Rabbits available in a single group. Group I was considered as standard (without any treatment). Osthole loaded MEBG and control gel as applied and adhered to rabbit dorsal skin in group II and III, respectively. Formalin was then used as a common irritant and bound 1 hour before MEBG and control gel application. Experimentation was performed for 7 days among all three groups. Osthole loaded MEBG and control gel was applied and adhered repeatedly once daily for 7 days. Then the applied area was recorded using Vernier Caliper for edema (Soliman et al. 2010). To take consistent results, observations were taken in triplicate.

### Statistical Analysis

One-way ANOVA and the *t*-test were used to distinguish and analyze at $p < 0.05$. Values were calibrated continuously three times in triplicate. Data was shown using mean value + S.D.

## RESULTS AND DISCUSSION

### Selection of components for microemulsions

Table I shows the solubility data. Kukui oil (oil), Labrasol (surfactant), Transcutol-P (co-surfactant) and water were chosen as microemulsion components because of having relatively maximum solubility and also miscibility with other microemulsion components. Kukui oil, Labrasol, Transcutol-P, water and PBS pH 7.4 showed solubilities (mg/mL) of 36, 111, 155 and 0.012 respectively.

Greater dermal flux was noticed primarily due to higher microemulsion solubilizing capacity resulting in a higher drug concentration gradient across the skin. Therefore, Kukui oil was chosen as it has moisturizing and anti-oxidant characteristics. Chemically, it comprises poly and monounsaturated fatty acid, linoleic, linolenic and vitamins C, D and E, which act as permeation enhancers (Ako et al. 1993).

Labrasol exhibited the highest solubility for Osthole among all used surfactants. All the surfactants employed appertain to nonionic surfactants class because of their lesser toxicity. Labrasol, a nonionic hydrophilic surfactant with hydrophilic lipophilic balance (HLB) 14, showed maximum bioavailability and enhance solubility and drug permeation. Usually, a balanced blend of high and low HLB surfactants prepares a stable microemulsion that also presents maximum solubility. Transient negative interfacial tension and fluid interfacial film are hardly accomplished

**Table I. Solubility of Osthole in oils, surfactants and co-surfacatants, values presented are mean +SD (n=3).**

| | Components | Solubility (mg/mL) Mean ± SD |
|---|---|---|
| **Oils** | Sesame oil | 29 ± 0.60 |
| | Kukui oil | 46 ± 0.91 |
| | Soybean oil | 33 ± 0.63 |
| | Sunflower oil | 26 ± 0.53 |
| | Oleic acid | 17.90 ± 0.68 |
| | Labrafil M1944 | 24 ± 0.59 |
| | Linoleic acid | 29 ± 0.45 |
| | Labrafac | 28 ± 0.71 |
| | Triacetin | 32 ± 0.65 |
| | Peanut oil | 23 ± 0.49 |
| | Ethyl Oleate | 32 ± 0.56 |
| | Isopropyl myristate (IPM) | 35.99 ± 0.94 |
| | Glycerol trioleate | 10.55 ± 0.57 |
| **Surfactants** | Cremophore RH40 | 70 ± 0.53 |
| | Cremophore EL-35 | 68 ± 0.44 |
| | Kolliphore HS 15 | 98 ± 0.53 |
| | Kolliphore RH 40 | 81 ± 0.39 |
| | Labrasol | 111 ± 0.61 |
| | Tween 20 | 91 ± 0.62 |
| | Tween 80 | 85 ± 0.40 |
| **Co-surfactants** | Polyethylene 200 | 86 ± 0.63 |
| | Transcutol-P | 155 ± 0.54 |
| | Polyethylene 400 | 79 ± 0.59 |
| | Ethanol | 46 ± 0.69 |
| | Propylene glycol | 69 ± 0.39 |
| **Water** | Water | 0.012 ± 0.004 |

using a single surfactant; usually, adding a co-surfactant is necessary. The mixing of a co-surfactant reduces the interface blending stress. It allows the interfacial film sufficient flexibility for undertaking the different curvatures required to form microemulsion over a wide constitution range. Depending on amphiphilic nature, co-surfactant accrues considerably on the interfacial layer, increasing the interfacial film fluidity via penetrating into the surfactant mono-layer (He et al. 2010). Thus, co-surfactant chosen for this study was Transcutol-P with an HLB value of 4.2 and exhibited maximum solubility for Osthole. Transcutol-P showed the ability to form transparent and stable microemulsion (Shah et al. 2015). All chemicals employed were pharmaceutically acceptable and fell under the GRAS category.

## Construction of pseudoternary phase diagrams

Oil and Smix concentrations depended on the water uptake in microemulsion by trial and error method. Pseudoternary phase diagrams were drawn at Smix weight ratios of 1:1, 2:1 and 3:1 are shown in Figure 1(a,b,c). The shaded area established a translucent microemulsion region. The turbid area was depicted in the left region. Smix weight ratio of 1:1 showed maximum microemulsion region compared to weight ratios 2:1 and 3:1. All preparations were isotropic, stable, thermo-dynamically and precise. This diagram of weight ratio 1:1 was chosen and then loaded with the drug Osthole.

Pseudoternary phase diagrams were constructed to determine selected components concentration ranges for the presence of a microemulsion region. The clear, isotropic and low viscosity area was presented in the phase diagram with a single-phase translucent microemulsion region Figure 1(a,b,c). After a visual observation, the remaining area on the ternary diagrams was turbid and multi-phase conventional emulsions. There was no conversion of water into oil from oil/water microemulsion nature. There was a microemulsion narrowing region after increasing Smix weight ratios. It implies a decrease in the microemulsion region

with increasing and decreasing surfactant and co-surfactant concentrations, respectively (Zhu et al. 2008).

## Effects of MEBG

Various concentrations effects for polymer carbomer 940 over-optimized microemulsion $ME_1$ viscosity were observed via dispersing and swelling it at 0.50%, 0.75% and 1.00% concentrations, separately into the water (aqueous phase). After TEA addition drop by drop for modifying swelled polymer gel network bases pH, MEBG was formed after adding oily phase with different gel bases. Incorporation of carbomer 940 gel base yielded significant viscosity enhancement as microemulsion has little viscosity. MEBG viscosity with concentration at 0.50%, 0.75% and 1.00% carbomer 940 were 59000, 14000, 16100 cP, respectively. MEBG at 0.5% carbomer 940 depicted relatively greater fluidity. Carbomer 940 at 1% concentration resulting in higher gel viscosity. Lapasin reported carbomer 940 appropriateness at 1% concentration (Lapasin et al. 2001). Gel at 0.75% carbomer 940 concentration showed appropriate transdermal application fluidity. Thus carbomer 940 at 0.75% concentration was considered the optimal gel base for fabricating MEBG (Chen et al. 2007).

## Physicochemical characteristics

pH, viscosity, refractive index, poly dispersity index, average droplet size, and conductivity of 17 microemulsions were measured in the range of 5.29-5.83, 52-162 cP, 1.330-1.427, 0.116-0.388, 64-90 nm and 139-185 µS/cm, respectively. pH, viscosity, refractive index, poly dispersity index and conductivity values of optimized $ME_1$ were 5.76, 52 cP, 1.376, 0.116 and 185 µS/cm, respectively (Table II). AFM and zeta sizer determined the droplet size of 63.5 nm of optimized $ME_1$. AFM

**Table II. Characterization of Microemulsions.**

| Codes | pH | Conductivity σ (µS/cm) | Viscosity (cP) | Refractive Index | Poly Dispersity Index | Average Droplet Size (nm) |
|---|---|---|---|---|---|---|
| $ME_1$ | 5.76 | 185 ± 3.1 | 52 ± 0.45 | 1.376 | 0.116 ± 0.021 | 88 |
| $ME_2$ | 5.43 | 183 ± 2.1 | 57 ± 0.34 | 1.330 | 0.128 ± 0.027 | 84 |
| $ME_3$ | 5.78 | 140 ± 1.4 | 147 ± 0.41 | 1.394 | 0.353 ± 0.016 | 77 |
| $ME_4$ | 5.57 | 169 ± 1.7 | 99 ± 0.98 | 1.365 | 0.244 ± 0.014 | 78 |
| $ME_5$ | 5.69 | 165 ± 2.9 | 101 ± 0.77 | 1.366 | 0.252 ± 0.015 | 82 |
| $ME_6$ | 5.72 | 171 ± 2.5 | 99 ± 0.80 | 1.363 | 0.240 ± 0.028 | 70 |
| $ME_7$ | 5.27 | 175 ± 3.5 | 64 ± 0.55 | 1.366 | 0.152 ± 0.010 | 64 |
| $ME_8$ | 5.52 | 162 ± 1.1 | 112 ± 0.63 | 1.380 | 0.280 ± 0.026 | 76 |
| $ME_9$ | 5.67 | 164 ± 2.6 | 106 ± 0.70 | 1.358 | 0.257 ± 0.024 | 72 |
| $ME_{10}$ | 5.63 | 157 ± 2.7 | 109 ± 0.61 | 1.382 | 0.286 ± 0.013 | 74 |
| $ME_{11}$ | 5.79 | 151 ± 2.8 | 142 ± 0.53 | 1.413 | 0.344 ± 0.011 | 66 |
| $ME_{12}$ | 5.66 | 165 ± 1.3 | 109 ± 0.67 | 3.370 | 0.267 ± 0.022 | 79 |
| $ME_{13}$ | 5.77 | 147 ± 1.6 | 155 ± 0.36 | 1.421 | 0.368 ± 0.020 | 85 |
| $ME_{14}$ | 5.80 | 162 ± 2.5 | 109 ± 0.65 | 3.721 | 0.276 ± 0.019 | 88 |
| $ME_{15}$ | 5.81 | 139 ± 3.5 | 162 ± 0.78 | 1.427 | 0.388 ± 0.017 | 71 |
| $ME_{16}$ | 5.45 | 182 ± 1.5 | 63 ± 0.50 | 1.333 | 0.141 ± 0.012 | 89 |
| $ME_{17}$ | 5.74 | 173 ± 1.3 | 93 ± 0.75 | 1.361 | 0.226 ± 0.023 | 75 |

findings are represented in Figure 2. Zeta potential was -0.159 mV, which showed the value was near neutral.

pH decreased for all 17 microemulsion preparations as the water was consecutively increasing. At higher water concentrations, organic acid ionization is enhanced, producing different protons in solution and thereby reducing pH. Therefore, pH valid parameter for inspecting skin safety. Despite this, microemulsion pH values were within physiological range and considered safe for skin with little interference till MEBG was also prepared for further adjusting microemulsion pH that is entirely safe and distinguishable to transdermal applications to skin (Naeem et al. 2019).

The calibrated viscosity increased at maximum oil levels. Enhancing water was anticipated to minimize viscosity, although minimizing surfactant concentration and co-surfactant enhanced the interfacial tension between two phases, water and oil. There was an increase in viscosity as decreasing interfacial area and then enhanced internal domain size. Incorporating transcutol-P (co-surfactant) reveals in changing flow to simple Newtonian. Viscosity was enhanced by Smix ratio as 3:1 > 2:1 > 1:1. Smix at 3:1 exhibited the highest viscosity (Shah et al. 2015).

Viscosity is considered a flow characteristic while Newtonian flow aims at microemulsions. Microemulsion viscosity is dependent on oil, surfactant, co-surfactant and water components

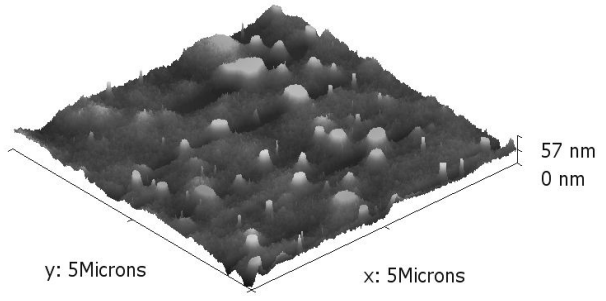


**Figure 2. AFM image of Osthole microemulsion.**

concentrations. Because of low viscosity, microemulsion did not adhere to the skin as it shows little viscosity. Hence its viscosity was enhanced after incorporating $ME_1$ over polymer carbomer 940 gel bases for producing sustained and therapeutic effects for long time. So, the microemulsion and MEBG were believed to be the best vehicle and dosage forms for Osthole drug transdermal delivery (Naeem et al. 2017).

It is defined as free ions movement in microemulsion. Figure 1(a,b,c) showed an extensive range of stable, isotropic and little viscosity microemulsions that increased water concentration. It depicts water concentration effects on microemulsion conductivity. After water concentration increased, the electrical conductivity also enhanced and reduced after reducing water concentration. Conductivity values describe the formed microemulsion in nature oil/water as it has water as a continuous phase.

It is validated for a robust correlation between microemulsion structure and their conductivity behavior. Conductivity is consequently a fruitful parameter for evaluating the properties of the microemulsion. This modulation is demonstrated with the creation of bi-continuous structures, which have ultra-low kind of interfacial tension. Conductivity values of greater than one $\mu Scm^{-1}$ are characteristic of the solution or bi-continuous type of microemulsions, whereabouts the existence of water in continuous pseudo-phase results in measuring conductivity. These dynamic structures comprise oil and water, pseudo domains that can quickly exchange. Its values will be poor when using oil as a continuous phase and vital when using water as a constant phase (Hathout et al. 2010).

It is for microemulsions represent the smaller scattering angle, and its value increased with increasing concentration of oil and surfactants.

It was also found that more concentrations of oil and surfactant results in increased droplet size because it shows a greater scattering angle and then increases the refractive index. Refractive indexes check the clarity, isotropic and transparency of microemulsion with the light scattering principle that entails applying the incident beam of radiation to microemulsion. Afterwards, it can aid in locating the intensity and angle of the scattered beam. Enlarge and small droplets of microemulsion have large and small scattering angles, respectively (Gannu & Rao 2012).

It was smaller, uniformly distributed (deflocculated) and within the microemulsion range. All poly-dispersity index values were found to be smaller than 0.5, which demonstrates the homogeneity and narrow size distribution of droplets. Zeta potential value represents the stability of microemulsion containing non-ionic surfactants is independent of zeta potential. Small droplet size gives excellent strength against sedimentation, coalescence and flocculation. Values of poly-dispersity index near to one show the droplet size come with significant uncertainty. Smaller droplets showed negative zeta potential and deflocculation property with uniform distribution (Gannu et al. 2010).

The droplets found were almost spherical with smooth surface and uniform distribution. There was no adhesion or aggregation among droplets of microemulsion because they are uniformly distributed and deflocculated into the system (Figure 2). AFM is a primary indicator to distinguish topographical aspects of droplets submerged in liquid by interpreting the microemulsion shape, morphology and size. It is also used to determine the microstructure of microemulsion. The main advantage of AFM for droplet characterization is the direct measurements of volume and 3D display (Fanun et al. 2010).

### *In Vitro* Skin Permeation Experiments

Permeation studies for 17 microemulsions, MEBG and control gel preparations were conducted on Rabbit skin (Table III). Permeation parameters ($Q_{24}$, flux and lag time) were determined for all preparations. $Q_{24}$, flux and lag time values were 5889 - 10101 µg, 111 - 147 µg/cm$^2$/h and 0.18 - 0.46 hr, respectively, for all 17 microemulsion preparations. $ME_1$ exhibited higher $Q_{24}$ (10101 µg) and flux (147 µg/cm$^2$/h) values and lowest lag time (0.18 hr) values. MEBG exhibited 9001 µg, 143 µg/cm$^2$/h and 0.21 hr values for $Q_{24}$, flux and lag time, respectively. Control gel preparation exhibited 2001 µg, 45 µg/cm$^2$/h and 1.6 hr values for $Q_{24}$, flux and lag time, respectively.

The permeation mechanism of $ME_1$, MEBG and Control gel was shown in Figure 3. Regarding Osthole optimum microemulsion, a significant reduction in $Q_{24}$ was observed after mixing of $ME_7$ with the Carbomer 940 gel base. Additionally, the lag time for formulating MEBG was in the range of 0.21 hr significantly higher than the $ME_1$ lag time. The optimized $ME_1$ enhancement ratio was 5.2 times higher than the control formulation. The enhancement ratio of MEBG was 3.4 times higher than the control formulation. *In vitro* studies of $ME_1$, MEBG and control gel formulations are shown in Figure 3, representing how the permeation parameters are considerably influenced using varying microemulsion composition.

### Formulation optimization

Independent variables and their responses are shown in Table IV. 3D contour and response surface plots are shown in Figure 4(a,b,c,d,e,f).

**Table III.** Variables and observed responses in Box Behnken Design for microemulsions.

| Microemulsion | Independent variables | | | Dependent variables | | | Enhance ment Ratio |
|---|---|---|---|---|---|---|---|
| | Oil $X_1$ (g) | Smix $X_2$ (g) | Water $X_3$ (g) | $Q_{24}$ $Y_1$ (µg) | Flux $Y_2$ µg/ $cm^2/h$ | Lag Time $Y_3$ (hour) | |
| ME1 | -1 | 0 | +1 | 10101 | 147 | 0.18 | 3.27 |
| ME2 | 0 | +1 | +1 | 7871 | 119 | 0.33 | 2.64 |
| ME3 | 0 | +1 | -1 | 7955 | 121 | 0.35 | 2.69 |
| ME4 | 0 | 0 | 0 | 8143 | 125 | 0.32 | 2.78 |
| ME5 | 0 | 0 | 0 | 8253 | 127 | 0.30 | 2.82 |
| ME6 | -1 | -1 | 0 | 8820 | 140 | 0.20 | 3.11 |
| ME7 | +1 | 0 | +1 | 7232 | 118 | 0.35 | 2.62 |
| ME8 | +1 | +1 | 0 | 5889 | 111 | 0.46 | 2.47 |
| ME9 | 0 | 0 | 0 | 8240 | 127 | 0.32 | 2.82 |
| ME10 | +1 | -1 | 0 | 6693 | 116 | 0.39 | 2.58 |
| ME11 | -1 | 0 | -1 | 8940 | 143 | 0.21 | 3.18 |
| ME12 | 0 | 0 | 0 | 8430 | 131 | 0.26 | 2.91 |
| ME13 | 0 | -1 | -1 | 8071 | 123 | 0.35 | 2.73 |
| ME14 | 0 | 0 | 0 | 8431 | 132 | 0.24 | 2.93 |
| ME15 | +1 | 0 | -1 | 6323 | 115 | 0.38 | 2.56 |
| ME16 | 0 | -1 | +1 | 8680 | 121 | 0.35 | 2.69 |
| ME17 | -1 | +1 | 0 | 8751 | 136 | 0.22 | 3.02 |

| Independent variables | Levels used, actual (coded) | | |
|---|---|---|---|
| | Low (-1) | Medium (0) | High (+1) |
| Oil (g) | 5 | 10 | 15 |
| Smix (g) | 35 | 42.5 | 50 |
| Water (g) | 40 | 47.5 | 55 |

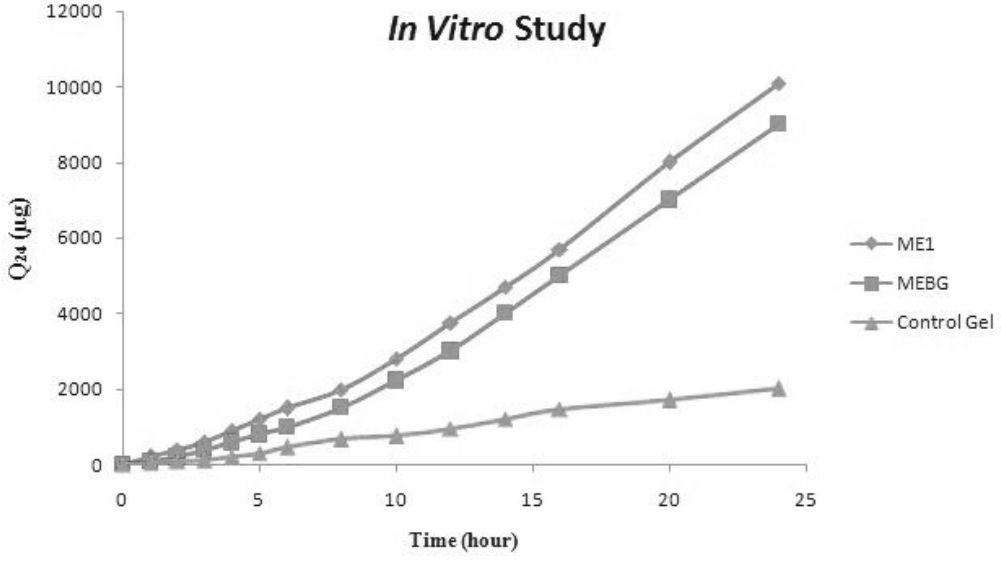


**Figure 3.** *In vitro* permeation profiles of Osthole ($ME_1$, MEBG and Control Gel) (n = 3).

Mathematical quadratic equations were created using DES.

When oil and Smix concentrations were used at -1 or 0 and 0 or +1, respectively, it elaborates significantly higher $Q_{24}$ ($Y_1$ = 7871 - 10101 µg) and flux ($Y_2$ = 119 - 147 µg/cm$^2$/h) values. If Smix was utilized at -1 to +1, it elaborates $Q_{24}$, flux and lag time as 5889 - 10101 µg, 111 - 147 µg/cm$^2$/h, 0.18 - 0.46 hr, respectively. Enhanced drug permeation is found at low, medium and high levels for oil, Smix and water, respectively. Lower drug permeation is determined at the high, high and medium levels of oil, Smix and water. Formulation variables and their levels at different combinations were utilized for estimating quantitative effects for $Q_{24}$, flux and lag time (Gannu et al. 2010). DES was employed for calculating response surface plots by

**Table IV. Composition of checkpoint formulations, the predicted and experimental values of response variables and percentage prediction error.**

| No. | Oil | Smix | Water | Response variables | Predicted value | Experimental value | Percentage prediction error |
|---|---|---|---|---|---|---|---|
| 1 | -1 | 0 | +1 | $Y_1$ | 9832 | 9980 | 1.482 |
| | | | | $Y_2$ | 144 | 145 | 0.689 |
| | | | | $Y_3$ | 0.198 | 0.190 | 0.502 |
| 2 | 0 | +1 | +1 | $Y_1$ | 9797 | 9780 | 0.020 |
| | | | | $Y_2$ | 144.62 | 144.01 | 0.076 |
| | | | | $Y_3$ | 0.200 | 0.205 | 0.497 |
| 3 | 0 | +1 | -1 | $Y_1$ | 9831 | 9820 | 0.101 |
| | | | | $Y_2$ | 144.61 | 144.40 | 0.062 |
| | | | | $Y_3$ | 0.198 | 0.197 | 0.502 |
| 4 | 0 | 0 | 0 | $Y_1$ | 9750 | 9760 | 0.102 |
| | | | | $Y_2$ | 144 | 144.05 | 0.034 |
| | | | | $Y_3$ | 0.200 | 0.201 | 0.497 |
| 5 | -1 | -1 | 0 | $Y_1$ | 5770 | 5780 | 0.173 |
| | | | | $Y_2$ | 144.6 | 144.1 | 0.138 |
| | | | | $Y_3$ | 0.200 | 0.205 | 0.990 |
| 6 | +1 | 0 | +1 | $Y_1$ | 9714 | 9720 | 0.061 |
| | | | | $Y_2$ | 144.9 | 144.3 | 0.068 |
| | | | | $Y_3$ | 0.200 | 0.205 | 1.477 |
| 7 | +1 | +1 | 0 | $Y_1$ | 9163 | 5899 | 0.076 |
| | | | | $Y_2$ | 143 | 145 | 0.694 |
| | | | | $Y_3$ | 0.2189 | 0.219 | 0.045 |
| 8 | +1 | -1 | 0 | $Y_1$ | 9203 | 9210 | 0.076 |
| | | | | $Y_2$ | 144.8 | 144.9 | 0.069 |
| | | | | $Y_3$ | 0.213 | 0.215 | 0.930 |
| 9 | -1 | 0 | -1 | $Y_1$ | 9589 | 9595 | 0.062 |
| | | | | $Y_2$ | 142 | 142.2 | 0.140 |
| | | | | $Y_3$ | 0.204 | 0.200 | 0.970 |
| 10 | +1 | 0 | -1 | $Y_1$ | 9366 | 9320 | 0.149 |
| | | | | $Y_2$ | 145 | 144.7 | 0.684 |
| | | | | $Y_3$ | 0.208 | 0.205 | 0.478 |

implementing factor levels values. The model was shown as follows:

$$Y_1(Q_{24}) = 8387 - 1288X_1 - 224X_2 + 303X_3 - 173X_1X_2 - 11X_1X_3 - 173X_2X_3 - 398X_1^2 - 350X_2^2 + 207X_3^2$$

$$Y_2(\text{Flux}) = 128 - 13X_1 - 1.63X_2 + 0.37X_3 - 0.25X_1X_2 - 0.25X_1X_3 + 0.001X_2X_3 + 3.55X_1^2 - 6.20X_2^2 - 1.20X_3^2$$

$$Y_3(\text{Lag time}) = 0.31 + 0.1X_1 + 8.75X_2 - 1.0X_3$$

## Thermodynamic Stability Study

Visual examination exhibited that the optimized formulations were stable when subjected to centrifugation and freeze-thaw cycles. Osthole concentration of optimized $ME_1$ and MEBG were 98% and 98.2%, respectively, for six months. Results exhibited the Osthole remained stable for the study period. Optimized $ME_1$ and MEBG exhibited $Q_{24}$ of 9899 µg and 8838 µg, respectively, for Osthole permeated in 24 hr. The optimized $ME_1$and MEBG, flux values were 146.5 and 142.5 µg/$cm^2$/h, respectively. The results of observations did not depict a significant difference ($p > 0.05$) for permeation release rate compared to initial permeation studies representing that both formulations were stable. No substantial change has been noticed in visual clarity, transparency, phase separation, color change, non-grittiness and drug content (Aggarwal et al. 2013).

## Skin irritation study

Skin erythema index is an arbitrary unit determined using Mexameter. Its values before and after the MEBG application were 215 - 280 and 225 - 290, respectively. No change in skin erythema was noticed after the MEBG application representing it non-irritant.

Although, all substances utilized for the microemulsion preparations are considered under the Generally Regarded as Safe (GRAS) category, all substances concentrations are crucial for such preparations. For example, a large surfactant concentration causes skin irritation. Therefore, a skin irritation test was performed to check substance concentrations employed for microemulsion preparation. In addition, this test was used to find any optimized microemulsion localized skin reaction.

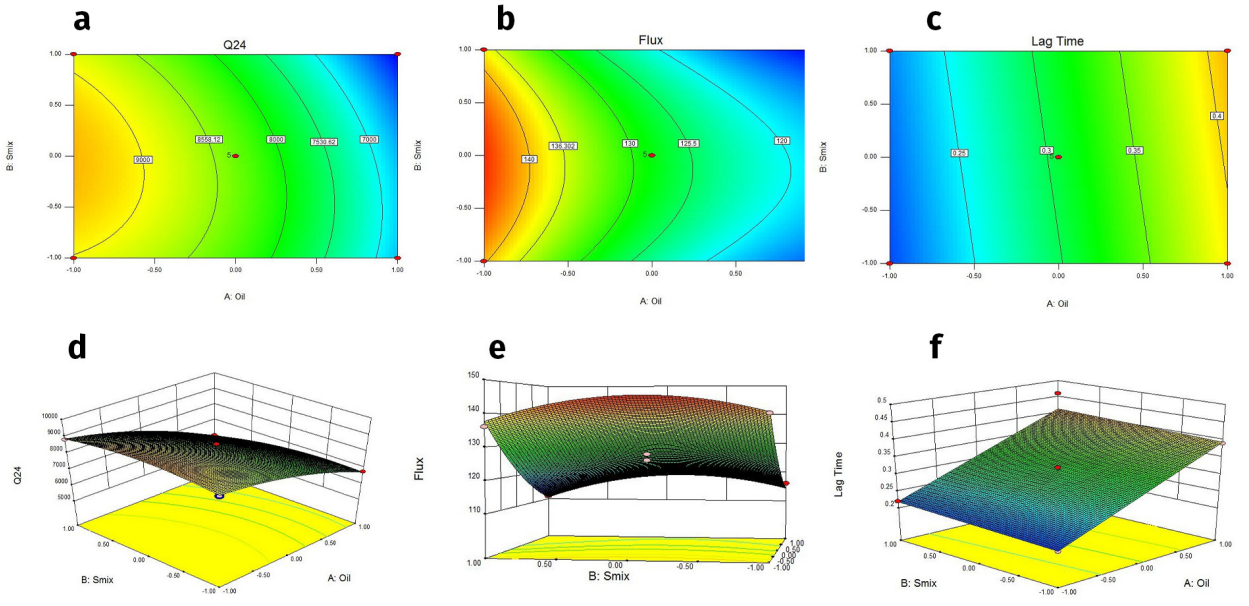


**Figure 4. Contour plot showing effects (a) $Q_{24}$ (b) Flux (c) Lag Time corresponding response surface plots (d - f).**

Skin erythema index shows optimized formulations for skin irritation. In the current study, an insignificant difference was present for skin erythema index measured before and after MEBG application. Furthermore, the skin was safe with no irritation (Naeem et al. 2017).

### Anti-Inflammatory study

Edema induced using the Formalin model was employed for distinguishing anti-inflammatory activity for Osthole MEBG and conventional gel. A significant difference was observed in comparing edema percent inhibition for MEBG (90%) and control gel (50%) as compared with standard (without using gel) (Figure 5).

When MEBG and control gel was applied to the skin against inflammation it was noticed that the edema was relatively less when compared with control gel, which showed that Osthole permeation via skin showed anti-inflammatory activity. For comparing the anti-inflammatory activity of MEBG and control gel, the edema percent inhibition was illustrated in Figure 5. MEBG was more efficacious and effective over reaching control gel throughout the study, depicting the Osthole addition to MEBG potentiate the anti-inflammatory activity (Soliman et al. 2010).

## CONCLUSION

Microemulsion increased Osthole solubility by using high solubility and miscibility components. These components extracted the lipids and enhanced the permeability through Rabbit skin. RDM was applied using BBD to optimize of independent variables for predicting dependent variables via a quadratic model considered the best fit model. MEBG was fabricated to enhance $ME_1$ transdermal adhesion with skin by extending its retention time. Results exhibited that MEBG was non-irritating and did-not cause erythema. The anti-inflammatory study showed a significant difference in percent inhibition of edema than with control gel. *In vivo* bioavailability results demonstrated maximum permeation of Osthole using MEBG than oral suspension. This system could further be investigated for other biopharmaceutical classification systems (BCS) II.

### Acknowledgments

The authors would like to thank Faculty of Pharmacy and Alternative Medicine, the Islamia University of

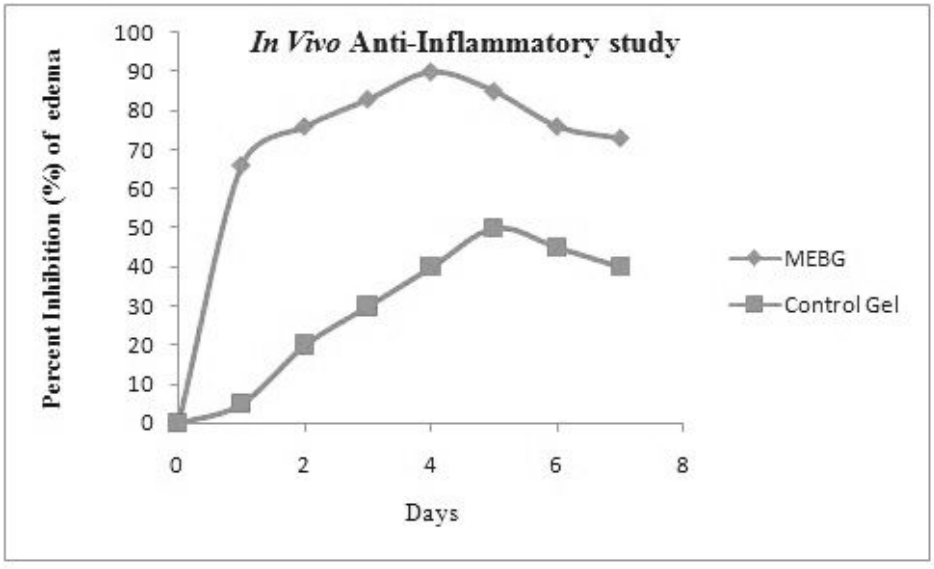


**Figure 5. Anti-inflammatory activity of MEBG and control gel.**

Bahawalpur, Bahawalpur, Pakistan, for providing Reserach Laboratory Services. The participation of authors Abdulhakeem S. Alamri and Charis M. Galanakis was supported by Taif University Researchers Supporting Project (TURSP-HC2023/4), Taif, Saudi Arabia.

## REFERENCES

AGGARWAL N, GOINDI S & KHURANA R. 2013. Formulation, characterization and evaluation of an optimized microemulsion formulation of griseofulvin for topical application. Colloids Surf B Biointerfaces 105: 158-166.

AKO H, FUJIKAWA L & GRAY D. 1993. Emollient action of kukui nut oil. J Soc Cosmet Chem 44(5): 42-57.

BOX GE & BEHNKEN DW. 1960. Some new three level designs for the study of quantitative variables. Technometrics. 2(4): 455-475.

CHEN H, CHANG X, DU D, LI J, XU H & YANG X. 2006. Microemulsion-based hydrogel formulation of ibuprofen for topical delivery. Int J Pharm 315(1-2): 52-58.

CHEN H, MOU D, DU D, CHANG X, ZHU D, LIU J, XU H & YANG X. 2007. Hydrogel-thickened microemulsion for topical administration of drug molecule at an extremely low concentration. Int J Pharm 341(1-2): 78-84.

FANUN M, MAKHARZA S & SOWWAN M. 2010. UV-Visible and AFM Studies of Nonionic Microemulsions. J Dispers Sci Technol 31(4): 501-511.

GANNU R, PALEM CR, YAMSANI VV, YAMSANI SK & YAMSANI MR. 2010. Enhanced bioavailability of lacidipine via microemulsion based transdermal gels: formulation optimization, ex vivo and in vivo characterization. Int J Pharm 388(1-2): 231-241.

GANNU R & RAO YM. 2012. Formulation optimization and evaluation of microemulsion based transdermal therapeutic system for nitrendipine. J Dispers Sci Technol 33(2): 223-233.

HATHOUT RM, WOODMAN TJ, MANSOUR S, MORTADA ND, GENEIDI AS & GUY RH. 2010. Microemulsion formulations for the transdermal delivery of testosterone. Eur J Pharm Sci 40(3): 188-196.

HE C, HU Y, YIN L, TANG C & YIN C. 2010. Effects of particle size and surface charge on cellular uptake and biodistribution of polymeric nanoparticles. Biomater 31(13): 3657-3666.

JENSEN WA. 2017. Response surface methodology: process and product optimization using designed experiments. J Qual Technol 49(2): 186-188.

KHURI AI & MUKHOPADHYAY S. 2010. Response surface methodology. Wiley Interdiscip Rev Comput Stat 2(2): 128-149.

LAPASIN R, GRASSI M & COCEANI N. 2001. Effects of polymer addition on the rheology of o/w microemulsions. Rheol Acta 40: 185-192.

LAWRENCE MJ & REES GD. 2000. Microemulsion-based media as novel drug delivery systems. Adv Drug Deliv Rev 45(1): 89-121.

LIAO PC ET AL. 2010. Osthole regulates inflammatory mediator expression through modulating NF-κB, mitogen-activated protein kinases, protein kinase C, and reactive oxygen species. J Agric Food Chem 58(19): 10445-10451.

NAEEM M, NAWAZ Z, IQBAL T, HUSSAIN S, YOUSUF M, KHAN JA, IDREES HA & ALI A. 2019. Microemulsion and microemulsion based gel of Zaleplon for transdermal delivery: preparation, optimization, and evaluation. Acta Pol Pharm 76(3): 543-561.

NAEEM M, PERVAIZ F, NAWAZ Z, YOUSUF M, ALI A, KHALID N & KHAN JA 2017. A quality by design approach: fabrication, characterization and evaluation of optimized transdermal therapeutic system for anti-rheumatic Lornoxicam. Acta Pol Pharm 74(1): 249-266.

NAEEM M, RAHMAN NU, KHAN JA, SEHTI A & NAWAZ Z. 2013. Development and optimization of microemulsion formulation using Box-Behnken design for enhanced transdermal delivery of Lornoxicam. Lat Am J Pharm 32(8): 1196-1204.

NAEEM M, RAHMAN NU, TAVARES G, BARBOSA SF, CHACRA NB, LOEBENBERG R & SARFRAZ MK. 2015. Physicochemical, in vitro and in vivo evaluation of flurbiprofen microemulsion. An Acad Bras Cienc 87: 1823-1831.

SAHOO S, PANI NR & SAHOO SK. 2014. Microemulsion based topical hydrogel of sertaconazole: Formulation, characterization and evaluation. Colloids Surf B Biointerfaces 120: 193-199.

SHAH BM, MISRA M, SHISHOO CJ & PADH H. 2015. Nose to brain microemulsion-based drug delivery system of rivastigmine: formulation and ex-vivo characterization. Drug Deliv 22(7): 918-930.

SOLIMAN SM, MALAK NA, EL-GAZAYERLY ON & REHIM AA. 2010. Formulation of microemulsion gel systems for transdermal delivery of celecoxib: In vitro permeation, anti-inflammatory activity and skin irritation tests. Drug Discov Ther 4(6): 459-471.

YOU L, FENG S, AN R & WANG X. 2009. Osthole: a promising lead compound for drug discovery from a traditional Chinese medicine (TCM). Nat Prod Commun 4(2): 297-302.

ZHU W, GUO C, YU A, GAO Y, CAO F & ZHAI G. 2009. Microemulsion-based hydrogel formulation of penciclovir for topical delivery. Int J Pharm 378(1-2): 152-158.

ZHU W, YU A, WANG W, DONG R, WU J & ZHAI G. 2008. Formulation design of microemulsion for dermal delivery of penciclovir. Int J Pharm 360(1-2): 184-190.

**How to cite**

NAEEM M, IQBAL T, YOUSUF M, NAWAZ Z, HUSSAIN S, ALAMRI AS, GALANAKIS CM & ALI A. 2023. Preparation, optimization and evaluation of Osthole transdermal therapeutic system. An Acad Bras Cienc 95: e20221023. DOI 10.1590/0001-3765202320221023.

*Manuscript received on November 30, 2022; accepted for publication on May 24, 2023*

**MUHAMMAD NAEEM**[1]
https://orcid.org/0000-0003-3368-8270

**TANIYA IQBAL**[2]
https://orcid.org/0000-0003-1061-528X

**MUHAMMAD YOUSUF**[3]
https://orcid.org/0009-0003-8292-8450

**ZARQA NAWAZ**[4]
https://orcid.org/0000-0003-4251-3069

**SAJJAD HUSSAIN**[5]
https://orcid.org/0000-0003-0635-1461

**ABDULHAKEEM S. ALAMRI**[6,7]
https://orcid.org/0000-0003-3174-0434

**CHARIS M. GALANAKIS**[8,9,10]
https://orcid.org/0000-0001-5194-0818

**ATIF ALI**[11]
https://orcid.org/0000-0002-7779-5804

[1]Shah Abdul Latif University, Department of Pharmacy, 66020, Khairpur, Sindh, Pakistan

[2]Bahauddin Zakariya University, Institute of Chemical Sciences, 60800, Multan, Punjab, Pakistan

[3]Peoples University of Medical and Health Sciences for Women, Institute of Pharmaceutical Sciences, 67480, Nawabshah, Sindh, Pakistan

[4]The Women University, Department of Chemistry, 66000, Multan, Punjab, Pakistan

[5]University of Agriculture, Department of Zoology, 03802, Faisalabad, Punjab, Pakistan

[6]Taif University, College of Applied Medical Sciences, Department of Clinical Laboratory Sciences, 21944, Taif, Saudi Arabia

[7]Taif University, Centre of Biomedical Sciences Research (CBSR), Deanship of Scientific Research, 21944, Saudi Arabia

[8]Galanakis Laboratories, Department of Research & Innovation, Skalidi 34, GR-73131, Chania, Greece

[9]Taif University, College of Science, Department of Biology, 21944, Taif, Saudi Arabia

[10]Food Waste Recovery Group, ISEKI Food Association, 56/18-19, 1070, Vienna, Austria

[11]COMSATS University Islamabad, Department of Pharmacy, Abbottabad Campus, 22060, Abbottabad, Pakistan

Correspondence to: **Muhammad Naeem**
*E-mail: naeem.mahar@salu.edu.com*

## Author contributions

Muhammad Naeem designed the idea, performed the practical and characterizes the data and wrote up the manuscript. Taniya Iqbal performed the analysis. Muhammad Yousuf and Atif Ali coordinate for characterization. Zarqa Nawaz and Sajjad Hussain performed statistical analysis. Abdulhakeem S. Alamri and Charis M. Galanakis cooperate for proofreading.